



# Electronic structure of $f^1$ actinide complexes. Part 3 of [1]. Quasi-relativistic density functional calculations of the optical transition energies of $\text{PaX}_6^{2-}$ ( $X=\text{F}, \text{Cl}, \text{Br}, \text{I}$ )

Nikolas Kaltsoyannis\*

*Department of Chemistry, University College London, 20 Gordon Street, London WC1H 0AJ, England*

## Abstract

The four  $f \rightarrow f$  transition energies of the single  $5f$ -based electron of  $\text{PaX}_6^{2-}$  ( $X=\text{F}, \text{Cl}, \text{Br}, \text{I}$ ) have been calculated using quasi-relativistic local density functional theory. Excellent agreement ( $<200 \text{ cm}^{-1}$ ) between theory and experiment is obtained for  $\text{PaCl}_6^{2-}$ ,  $\text{PaBr}_6^{2-}$  and  $\text{PaI}_6^{2-}$  by variation of the value of  $\alpha$  in the  $X\alpha$  exchange-only functional. In contrast, more sophisticated calculational methods including non-local corrections fail to reproduce the experiments well. The  $\text{PaF}_6^{2-}$  results are less impressive (up to  $1000 \text{ cm}^{-1}$  discrepancy), possibly due to non-aufbau orbital occupations for certain values of  $\alpha$ . The values of  $\alpha$  employed lie in the range  $0.79$ – $0.85$ , somewhat higher than the most widely used value of  $0.7$ . The theoretical basis for using such values is discussed. © 1998 Elsevier Science S.A.

*Keywords:* Density functional theory; Optical transition energies; Actinides; Electronic structure

## 1. Introduction

The calculation of optical transition energies in open-shell molecules is one of the greatest challenges in electronic structure theory. This is particularly true in actinide-containing compounds as not only must relativistic effects [2–5] be taken into account but the large number of valence orbitals on actinide centres leads to a large number of closely spaced ligand field transitions that can be difficult to assign. ' $f^1$ ' complexes (in which the actinide atom is in a formal oxidation state one less than its 'group valence') are attractive targets for study as they contain only one metal-localised valence electron and the problems associated with multiple-electron configurations are therefore avoided. We have previously reported the results of relativistic local density functional calculations of the optical transition energies of  $\text{PaX}_6^{2-}$  ( $X=\text{F}, \text{Cl}, \text{Br}, \text{I}$ ),  $\text{UX}_6^-$  ( $X=\text{F}, \text{Cl}, \text{Br}$ ) and  $\text{NpF}_6$  [6] and, more recently,  $[\text{M}(\eta\text{-C}_5\text{H}_5)_3]$  ( $\text{M}=\text{Ce}, \text{Th}$ ) and  $[\text{Pa}(\eta\text{-C}_8\text{H}_8)_2]$  [1], in which we managed to reproduce experimental data with varying degrees of success. Not surprisingly, the agreement between experiment and theory worsened as the molecules under investigation increased in size. Thus, while our calculations reproduced the optical spectra of the

hexahalide anions rather well, somewhat poorer results were obtained for the organometallic compounds.

The eventual aim of this project is to establish a methodology that will allow us to reproduce  $f$ -element optical spectra quantitatively, so that we may assist in the interpretation of new experimental data. This contribution reports some recent efforts in pursuit of this goal, in which the value of  $\alpha$  in the so called  $X\alpha$  exchange-only local density functional is adjusted so as to reproduce as closely as possible the experimental transition energies of the single  $f$ -localised electron of  $\text{PaX}_6^{2-}$  ( $X=\text{F}, \text{Cl}, \text{Br}, \text{I}$ ).

## 2. Computational details

All calculations were performed with the Amsterdam Density Functional program suite [7,8]. Double-zeta Slater-type orbital valence basis sets were employed for all atoms (ADF Type II). Quasi-relativistic scalar frozen cores were used for all elements; Pa (5d), F (1s), Cl (2p), Br (3d) and I (4d). Relativistic core potentials were computed using the ADF auxiliary programme 'Dirac'. The  $X\alpha$  local density functional was employed, and the value of  $\alpha$  was adjusted as described in the main text. All molecular geometries were fully optimised, and confirmed as global energy minima by the observation of only positive eigenvalues in the Hessian matrices. Electronic transition ener-

\*Corresponding author. Tel.: (44-171) 387-7050; fax: (44-171) 380 7463; e-mail: n.kaltsoyannis@ucl.ac.uk

gies were computed using the transition state method [9,10]. Separate calculations were converged for each transition.

### 3. Preliminary considerations

The effects of relativity must be included in any theoretical study of the electronic structure of heavy element systems [2–5], particularly when quantitative agreement between experiment and theory is sought. There are two major consequences of relativity for the electronic structure of molecules containing actinide elements. The first is the significant modification of the actinide atom's valence atomic orbital (AO) energies as a result of the stabilisation of the inner core *s* and *p* electrons, which are moving at velocities that are appreciable fractions of the speed of light. The effect on the valence AOs is to contract slightly the *s* and *p* levels and to destabilise the more diffuse *d* and *f* functions, which experience reduced nuclear charge due to increased shielding by the *s* and *p* electrons.

The second consequence is the coupling of electronic intrinsic spin angular momentum with that imposed by orbital motion, an effect which is increasingly important for heavy element systems. All electronic states in actinide complexes are therefore properly characterised by non-integral angular momentum values, and must be described using double point group symmetry notation [5,11]. For the octahedral point group, the most significant effect of spin-orbit coupling is the lifting of the degeneracy of the *t* symmetry orbitals. The relationship between the spatial molecular orbitals (MOs) of the  $O_h$  point group and the spin-orbitals of the  $O_h^*$  double group is given in Table 1.

The relativistic methodology implemented in the Amsterdam Density Functional package is the so called quasi-relativistic approach of Ziegler et al. [12]. This is an extension of the first-order perturbation method described by Snijders et al. [13], and has proven superior when applied to systems containing very heavy elements (beyond, for example, gold) [12]. The first-order (in  $\alpha^2$ , where  $\alpha$  is in this case the fine structure constant) Pauli

Hamiltonian—which contains the mass–velocity and Darwin relativistic corrections, as well as a spin-orbit operator—is diagonalised in the space of the zeroth-order solutions, i.e. the non-relativistic basis set. Thus, the technique stops short of a solution to the full Dirac-Slater equation, but is appropriate for the study of the valence electronic structure of actinide-containing molecules.

### 4. Results and discussion

The promotion energies of the single metal 5*f*-based electron in  $\text{PaX}_6^{2-}$  ( $X = \text{F}, \text{Cl}, \text{Br}, \text{I}$ ) are represented pictorially in Fig. 1. In  $O_h$  symmetry, the seven *f* orbitals divide into three sets, of  $a_{2u}$ ,  $t_{2u}$  and  $t_{1u}$  symmetry (in order of decreasing stability) [14]. Spin-orbit coupling lifts the degeneracy of the *t* orbitals as set out in Table 1, with the result that, while a non-relativistic treatment of  $\text{PaX}_6^{2-}$  would predict two *f*→*f* transitions ( $a_{2u}$ → $t_{2u}$  and  $a_{2u}$ → $t_{1u}$ ), the relativistic calculations yield four higher lying *f*-based orbitals (and, thus, four possible transitions). The calculated transition energies are written in plain text on Fig. 1, with the available experimental data given in italicised parentheses.

With the exception of  $\text{PaF}_6^{2-}$ , the agreement between theory and experiment is excellent ( $<200 \text{ cm}^{-1}$ , or 0.025 eV) in all cases. The procedure followed to arrive at these data, however, is somewhat convoluted. Initially, sophisticated basis sets (valence triple-zeta with polarisation functions) were employed in conjunction with the local density functional of Vosko, Wilk and Nusair [15] and a variety of non-local (gradient) corrections to obtain optimised geometries for each  $\text{PaX}_6^{2-}$ . The transition energies of the single metal 5*f*-based electron were then calculated via the fractional occupancy transition state method due to Slater [9,10]. This process, however, gave poor agreement between theory and experiment ( $>1000 \text{ cm}^{-1}$  discrepancy) in all cases. It was therefore decided to revert to less sophisticated valence double-zeta basis sets in conjunction with the  $X\alpha$  local density functional, and to vary  $\alpha$  to bring theory and experiment into as close a match as possible. For each value of  $\alpha$  the geometry was optimised and the four transition energies calculated as described above. Table 2 lists the optimised Pa–halogen distances for the value of  $\alpha$  used in the transition state calculations, together with metal–halogen bond lengths obtained from the radii of  $\text{Pa}^{4+}$  and the halide anions [16,17]. Clearly the optimised bond lengths are considerably shorter than those estimated from ionic radii data. However, using the bond lengths estimated from ionic radii and then varying the value of  $\alpha$  produced much poorer transition energy agreement than that given in Fig. 1. In order to achieve a close match of theory and experiment for the transition energies, the Pa–*X* bond length had to first be optimised at the chosen  $\alpha$  value. Alteration of  $\alpha$  required reoptimisa-

Table 1  
Relationship between the irreducible representations of the single and double octahedral point groups

$O_h$	$O_h^*$
$a_{1g}$	$e_{1/2}^+$
$a_{2g}$	$e_{5/2}^+$
$e_g$	$g_{3/2}^+$
$t_{1g}$	$g_{3/2}^+ + e_{1/2}^+$
$t_{2g}$	$g_{3/2}^+ + e_{5/2}^+$
$a_{1u}$	$e_{1/2}^-$
$a_{2u}$	$e_{5/2}^-$
$e_u$	$g_{3/2}^-$
$t_{1u}$	$g_{3/2}^- + e_{1/2}^-$
$t_{2u}$	$g_{3/2}^- + e_{5/2}^-$

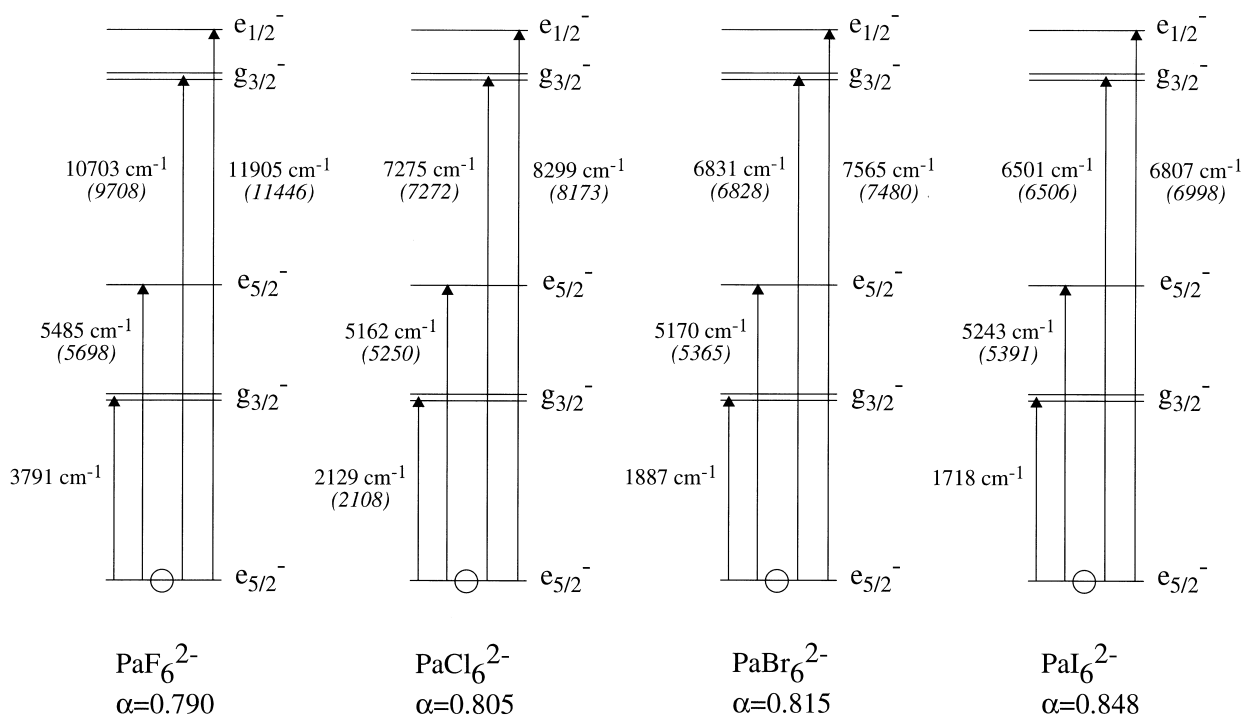


Fig. 1. Schematic representation of the energy levels of the molecular orbitals of predominant metal 5f character in  $\text{PaX}_6^{2-}$  ( $\text{X}=\text{F}, \text{Cl}, \text{Br}, \text{I}$ ). Vertical lines indicate the transitions of the single electron in the lower  $e_{5/2}^-$  orbital (represented by a circle) to the higher lying levels. Transition energies are given as calculated (experimental). The values of  $\alpha$  employed in the  $\text{X}\alpha$  exchange-only local density functional are given for each dianion. Experimental data are taken from references: [22] ( $\text{PaF}_6^{2-}$ ); [23] ( $\text{PaCl}_6^{2-}$ ); [24] ( $\text{PaBr}_6^{2-}$ ); and, [25] ( $\text{PaI}_6^{2-}$ ).

tion of the geometry before the transition energies were calculated.

The general trend in the data in Fig. 1 is for a given transition to become less energetic as the halogen becomes heavier. This reflects the greater metal–ligand bond length for the heavier halogens, which reduces the perturbation of the Pa 5f orbitals (i.e. the ligand field strength is smaller). Also of note is the much poorer match of theory and experiment for the  $\text{PaF}_6^{2-}$  transitions. This is not without precedent, in that our previous attempt to calculate  $\text{PaF}_6^{2-}$  was also less than satisfactory [6]. In the present calculations the discrepancy may well be due to an MO of  $e_{1/2}^+$  symmetry—of predominant Pa s character—in the same energy range as the 5f-based orbitals depicted in Fig. 1. Certain values of  $\alpha$  resulted in non-aufbau orbital occupations, i.e. the  $e_{1/2}^+$  level had a more negative eigenvalue than the  $e_{5/2}^-$  HOMO yet remained empty. The data given

for  $\text{PaF}_6^{2-}$  are the closest possible match with the experimental values when the aufbau principle is maintained in the ground and all four transition state calculations.

The reader may be forgiven for wondering if there is any justification for the seemingly arbitrary use of  $\alpha$  in the present calculations (apart, of course, from the fact that it works!). To answer this question, some theoretical background is required. The celebrated one-electron Kohn-Sham equation [18,19], on which much of density functional theory is based, may be written

$$\left( -\frac{1}{2}\nabla^2 + v(r) + \int \frac{\rho(r')}{|r-r'|} dr' + v_{xc}(r) \right) \phi_i = \epsilon_i \phi_i \quad (1)$$

where  $v(r)$  is the external potential acting on an electron in spin-orbital  $\phi_i$  at a point  $r$ ,  $\int (\rho(r')/|r-r'|)dr'$  is the Coulombic repulsion potential due to all of the other

Table 2  
Pa–X bond lengths (Å) in  $\text{PaX}_6^{2-}$  ( $\text{X}=\text{F}, \text{Cl}, \text{Br}, \text{I}$ )

	$\text{PaF}_6^{2-}$	$\text{PaCl}_6^{2-}$	$\text{PaBr}_6^{2-}$	$\text{PaI}_6^{2-}$
Calculated	2.15 ( $\alpha=0.790$ )	2.59 ( $\alpha=0.805$ )	2.72 ( $\alpha=0.815$ )	2.88 ( $\alpha=0.848$ )
'Experimental'	2.23	2.71	2.86	3.10

The value of  $\alpha$  in the exchange-only local density functional ( $\text{X}\alpha$ ) is given in parentheses. 'Experimental' values are estimated from Shannon's ionic radius of  $\text{Pa}^{4+}$  [16] and the Pauling radii of the halide ions [17].

electrons in the system and  $v_{xc}(r)$  is the exchange-correlation potential. This one-electron orbital treatment is rigorously correct and, provided we can construct the exchange-correlation potential, we can use the Kohn-Sham equation to determine the exact charge distribution and wavefunction of any electronic system of interest. In the Kohn-Sham approach,  $v_{xc}(r)$  is obtained from the exchange-correlation energy functional  $E_{xc}[\rho]$  as

$$v_{xc}(r) = \frac{\delta E_{xc}[\rho]}{\delta \rho(r)} \quad (2)$$

where the quantity  $[\delta E_{xc}[\rho]]/(\delta \rho(r))$  is the functional derivative of  $E_{xc}[\rho]$  with respect to the charge density  $\rho$  at point  $\rho$ . Among the simplest possible forms for  $E_{xc}[\rho]$  is the *exchange-only* functional of the homogeneous electron gas:

$$E_x[\rho] = -\frac{3}{4} \left( \frac{3}{\pi} \right)^{1/3} \int \rho(r)^{4/3} dr \quad (3)$$

Using this form for  $E_x[\rho]$  one obtains for  $v_x(r)$ :

$$v_x(r) = -\left( \frac{3\rho(r)}{\pi} \right)^{1/3} \quad (4)$$

Notice that Eq. (1) with  $v_{xc}(r)$  given by Eq. (4) is identical to the Hartree-Fock-Slater equation [20]

$$\left( -\frac{1}{2} \nabla^2 + v(r) + \int \frac{\rho(r')}{|r-r'|} dr' + v_{x\alpha}(r) \right) \phi_i = \varepsilon_i \phi_i \quad (5)$$

in which  $\alpha$  in  $v_{x\alpha}(r)$  (Eq. (6)) is set to 2/3:

$$v_{x\alpha}(r) = -\frac{3}{2} \alpha \left( \frac{3\rho(r)}{\pi} \right)^{1/3} \quad (6)$$

In Slater's original contribution,  $\alpha$  was set to 1. The use of different values of  $\alpha$  stems from the application of the uniform electron gas approximation in different places. Kohn and Sham apply it in the exchange *energy*, while Slater employs it in the exchange *potential*. The former approach emphasises the total energy whereas that of Slater concerns the one-electron equation. This ambiguity is the origin of the use of  $\alpha$  as an adjustable parameter in  $X\alpha$  calculations.

In most density functional packages, the default value for  $\alpha$  is 0.7. This is based on a large amount of collective experience with  $X\alpha$  calculations, going right back to Schwarz in 1972, who produced a table of recommended values of  $\alpha$  for all of the elements up to Nb, determined so that the optimised total  $X\alpha$  energy equals the Hartree-Fock energy [21]. The present study is not concerned with total energies, but with the one-electron energy spectrum. In that sense it is not surprising that the values of  $\alpha$  needed to

reproduce the electronic transition energies are some way from the Kohn and Sham total energy value of 2/3. Indeed the  $\alpha$  values used in this study lie almost exactly half way between the Kohn and Sham and Slater choices. Whether this proves to be a general feature of actinide optical spectra calculations, or a peculiarity of the present study, will play a central role in our search for a methodology that will allow us to reproduce f-element optical spectra quantitatively.

## Acknowledgements

I wish to thank the Royal Society for an equipment grant.

## References

- [1] N. Kaltsoyannis, B.E. Bursten, J. Organomet. Chem. 528 (1997) p. 19; part 2 of this article.
- [2] K.S. Pitzer, Acc. Chem. Res. 12 (1979) 271.
- [3] P. Pyykkö, Acc. Chem. Res. 8 (1979) 276.
- [4] P. Pyykkö, Chem. Rev. 88 (1988) 563.
- [5] N. Kaltsoyannis, J. Chem. Soc., Dalton Trans. (1997) 1.
- [6] N. Kaltsoyannis, B.E. Bursten, Inorg. Chem. 34 (1995) 2735.
- [7] G. te Velde, E.J. Baerends, J. Comp. Phys. 99 (1992) 84.
- [8] Amsterdam Density Functional (ADF) program suite 2.2, Department of Theoretical Chemistry, Vrije Universiteit, Amsterdam, 1997.
- [9] J.C. Slater, Adv. Quantum Chem. 6 (1972) 1.
- [10] J.S. Slater, The Calculation of Molecular Orbitals, Wiley, New York, 1979.
- [11] J.A. Salthouse, M.J. Ware, Point group character tables and related data, Cambridge University Press, London, 1972.
- [12] T. Ziegler, V. Tschinke, E.J. Baerends, J.G. Snijders, W. Ravenek, J. Phys. Chem. 93 (1989) 3050.
- [13] J.G. Snijders, E.J. Baerends, P. Ros, Mol. Phys. 38 (1979) 1909.
- [14] F.A. Cotton, Chemical Applications of Group Theory, 3rd ed., Wiley-Interscience, New York, 1991.
- [15] S.H. Vosko, L. Wilk, M. Nusair, Can. J. Phys. 58 (1980) 1200.
- [16] R.D. Shannon, Acta Cryst. A32 (1976) 751.
- [17] L. Pauling, The Nature of the Chemical Bond, Cornell University Press, Ithaca, NY, 1960.
- [18] W. Kohn, L.J. Sham, Phys. Rev. A 140 (1965) 1133.
- [19] R.G. Parr, W. Yang, Density-Functional Theory of Atoms and Molecules, OUP, Oxford, 1989.
- [20] J.S. Slater, Phys. Rev. 81 (1951) 385.
- [21] K. Schwarz, Phys. Rev. B5 (1972) 2466.
- [22] D. Brown, B. Whittaker, N.M. Edelstein, Inorg. Chem. 13 (1974) 1805.
- [23] D. Piehler, W.K. Kot, N.M. Edelstein, J. Chem. Phys. 94 (1991) 942.
- [24] N.M. Edelstein, D. Brown, B. Whittaker, Inorg. Chem. 13 (1974) 563.
- [25] D. Brown, P. Lidster, B. Whittaker, N.M. Edelstein, Inorg. Chem. 15 (1976) 511.